ChemBioChem

Chemistry Europe
European Chemical Societies Publishing
ChemBioChem

RESEARCH ARTICLE OPEN ACCESS

Expanding the Toolbox for Biocatalytic Halogenation by Identification and Characterization of Three Vanadium Chloroperoxidases

Sonja Schönrock | Nils Senge | Dirk Holtmann

Process Engineering in Life Sciences 2, Karlsruhe Institute of Technology, Karlsruhe, Germany

Correspondence: Dirk Holtmann (dirk.holtmann@kit.edu)

Received: 7 May 2026 | **Revised:** 7 May 2026 | **Accepted:** 12 May 2026

Keywords: biocatalysis | enzymatic halogenation | genome mining | haloperoxidase | oxidation

ABSTRACT

Halogenation reactions are essential for producing many fine and bulk chemicals. Vanadium-dependent chloroperoxidases (VCPOs) are promising biocatalysts for a more sustainable production of halogenated products because they are cofactor independent, use hydrogen peroxide (H_2O_2) as oxygen donor, tolerate high H_2O_2 concentrations, and catalyze all halogenations except fluorination. Despite their outstanding catalytic potential, few VCPOs have been identified yet, and detailed information on their catalytic characteristics is lacking. Here, we report the heterologous expression of three previously uncharacterized VCPOs in *Escherichia coli* and their validation. One of the enzymes was identified in the fungus *Curvularia clavata* (*Cc*VCPO). The other two were found in the bacteria *Crocinitomix catalasitica* (*Croc*VCPO) and in an uncultivated *Bacteroidetes* strain (U*b*VCPO) isolated from a water sample taken from lake Neuchâtel in Switzerland. These enzymes exhibit highly attractive features, including thermostability up to 40°C for the bromination reaction of monochlorodimedone (MCD), the highest chlorination turnover numbers reported to date for wild-type VCPOs for the variant U*b*VCPO, as well as increased enzyme activation at 40°C and in the presence of methanol or ethanol for the same enzyme variant. These findings significantly expand the VCPO toolbox and highlight their potential for sustainable halogenation processes.

1 | Introduction

Halogenation is a particularly effective tool for the activation of hydrocarbon molecules, thereby making them available for follow-up chemical conversion. For example, 50 % of all industrial chemicals and polymers contain chlorine atoms. The same applies to 22 % of Food and Drug Administration-approved small molecule drugs in 2024 and around 46 % of agrochemicals approved in recent years [1–3]. In pharmaceuticals, halogen groups can improve biological activities and stabilities such as enhanced absorption of drugs due to changes in lipophilicity [4]. In general, functionalization by halogenation enables a broad range of follow-up chemistry to produce complex molecules with new reactivities.

Direct insertion of halogens into organic compounds is often performed by heat, light, or by electrophilic aromatic substitution on aromatic rings. These reactions can be executed by reagents such as Selectfluor®, NBS/acid/MeOH, Ag^+/Br_2, or *N*, *N*'-dibromobenzene sulfonamide, leading to significant amounts of waste and consequently to a higher environmental impact [4]. A promising and environmentally friendlier alternative is the use of natural biocatalysts such as chloroperoxidases (CPOs) which can catalyze reactions with all halides except for fluorine and astatine [5, 6]. These kinds of biocatalysts are able to generate reactive hypohalites from inorganic salts. In particular, vanadium-dependend chloroperoxidases (VCPOs) demonstrate promising catalytic properties and tolerance to various reaction conditions. VCPOs use vanadate as cofactor in the catalytic center,

enabling the enzyme to oxidize halide ions to hypohalous acids. Unlike the heme in cytochrome P450 of heme-containing CPOs, the incorporated vanadate in VCPOs in the active site does not change its oxidation state during the catalysis and is therefore less prone to inactivation by hydrogen peroxide, hypohalous acid, or oxygen, making the VCPOs as biocatalysts even more favorable for catalysis [6–9].

VCPOs can convert strong aromatic carbon–hydrogen bonds (C–H) to halocarbons (C–X; X = Cl, Br, I) when vanadium as redox cofactor and hydrogen peroxide as cosubstrate are present [10]. The catalyzed reaction is an electrophilic halogenation [10]. First, the hydrogen peroxide is bound by the vanadate in the reaction pocket, resulting in a peroxovanadate intermediate and free water. Then, the halide ion gets oxidized which leads to a bound hypohalous acid [11]. In the vast majority of VCPOs, the hypohalous acid gets released into the immediate vicinity, where it reacts with electron-rich substrates close to the active site of the enzyme, resulting in a nonspecific halogenation. However, research has been conducted on several VCPO variants from *Streptomyces* bacteria which show regio- and stereospecificity. This specific catalysis is attributed to a lysine residue which carries the halogen radical from the cofactor to the substrate-binding site as well as to a shielded vanadate, which does not come into contact with the solvent [12]. This specific and directed conversion, however, is not seen in the majority of VCPOs yet and is highly dependent on the secondary structure in the active site of the enzyme [13, 14].

As compiled in detail in the recent review of Chen et al., only a limited number of enzymes belonging to the class of vanadium-dependent haloperoxidases have been identified to date, and even fewer have been well characterized [15]. Within this enzyme family, the number for VCPOs is yet smaller. The first ever characterized vanadium haloperoxidase (VHPO) was a vanadium bromoperoxidase from *Ascophyllum nodosum* [16]. Known VHPOs were isolated from microalgae, fungi, and bacteria. All identified VHPOs from algae belong to the group of either vanadium bromoperoxidases (VBPOs) or vanadium iodoperoxidases (VIPOs) [17]. A large share of VHPOs were found in bacteria. For example, in *Streptomyces* sp. and in the marine bacterium *Zobellia galactanivorans* some enzymes were characterized [18, 19]. Currently, only seven VHPOs from fungi are documented [15]. Among the subgroup of VCPOs, only three are well described regarding their ability to engage in halogenation reactions [15, 17]. The VCPO from *Curvularia inaequalis*, a terrestrial fungus, is well investigated [20]. The other two characterized enzymes are a VCPO from the fungus *Embellisia didymospora* and a VCPO from the marine fungus *Hortaea werneckii* [17, 21]. The *Ci*VCPO from *Curvularia inaequalis* is the most widely used VCPO to date. *Ci*VCPOs have been applied, e.g., in the enzymatic halogenation of phenols, indoles, acids, and activated aromatics; in addition, it is also reported that the enzyme assisted in the epoxidation of alkenes or chlorination of amines under suitable conditions by providing the necessary hypohalous acid [4, 6, 7, 10, 22–26]. Such products are of significant interest for the synthesis of fine chemicals, pharmaceuticals, and agrochemical intermediates.

However, limited knowledge of substrate specificity is a disadvantage of these enzymes, restricting the potential for industrial application. There is a need for a bigger variety of these VCPOs, more characterization data concerning the optimal reaction conditions for the biocatalysts and also data about their substrate specificity.

Although VCPOs show remarkable properties regarding stability against cofactor inactivation, higher temperatures and organic solvents, only a limited number of enzymes from this class are currently known and properly characterized. The aim of the current investigation was to extend the VCPO toolbox, paving the way for more sustainable, enzyme-based halogenation approaches in the future and, in the long term, enabling the development of biocatalysts for the activation of hydrocarbons and their conversion into valuable intermediates. In this study, the expansion of the VCPO group by three more enzymes is reported, which were heterologously expressed and characterized as VCPOs. One VCPO originates from the fungus *Curvularia clavata*. The other two are from bacterial strains: one from *Crocinitomix catalasitica* and the other from an uncultured *Bacteroidetes* strain that was part of a water sample from lake Neuchâtel in Switzerland.

2 | Results and Discussion

2.1 | Identification of Putative Vanadium-Dependent Chloroperoxidase Sequences

In cooperation with the external partner Proteineer GmbH, a screening for VCPO gene sequences was performed using the VCPO sequence from *Curvularia inaequalis* (*Ci*VCPO) as reference. Based on the provided dataset of DNA sequences by Proteineer GmbH, sequences were selected according to the parameters: amino acid sequence length, predicted thermostability and solubility, and topological similarity (TM-score). The underlying algorithms for this parameter-based DNA sequence search are subject to company confidentiality and therefore cannot be disclosed in detail. Additional parameters for the selection included the source of organism, their respective habitats, and the degree of sequence similarity to the reference enzyme *Ci*VCPO. As the screening tool from Proteineer GmbH showed sequences without introns, no additional screening for introns was performed for the hits with fungal origin. The final set of sequences was codon optimized for heterologous expression in *Escherichia coli*. Among the selected sequences, preliminary tests led to the identification of the three VCPOs presented here. One of these enzymes, *Cc*VCPO, originates from the fungus *Curvularia clavata*, which is in close relation to the reference enzyme *Ci*VCPO. This enzyme was first described by both, Zhang et al. and Loan et al. [27, 28]. Nevertheless, the reports focused on the catalysis of bromoform and enantioselectivity of sulfoxidation, lacking specific information of the properties to characterize this enzyme. The second enzyme, *Croc*VCPO, derived from the Flavobacterium *Crocinitomix catalasitica*. The third enzyme, referred to as U*b*VCPO, was isolated from an uncultured *Bacteroidetes* (U*b*) strain from a water sample.

2.2 | Classification as Vanadium-Dependent Chloroperoxidases

Halogenation assays with iodine, bromine, and chlorine (Figure 1) were performed to determine, if the identified putative

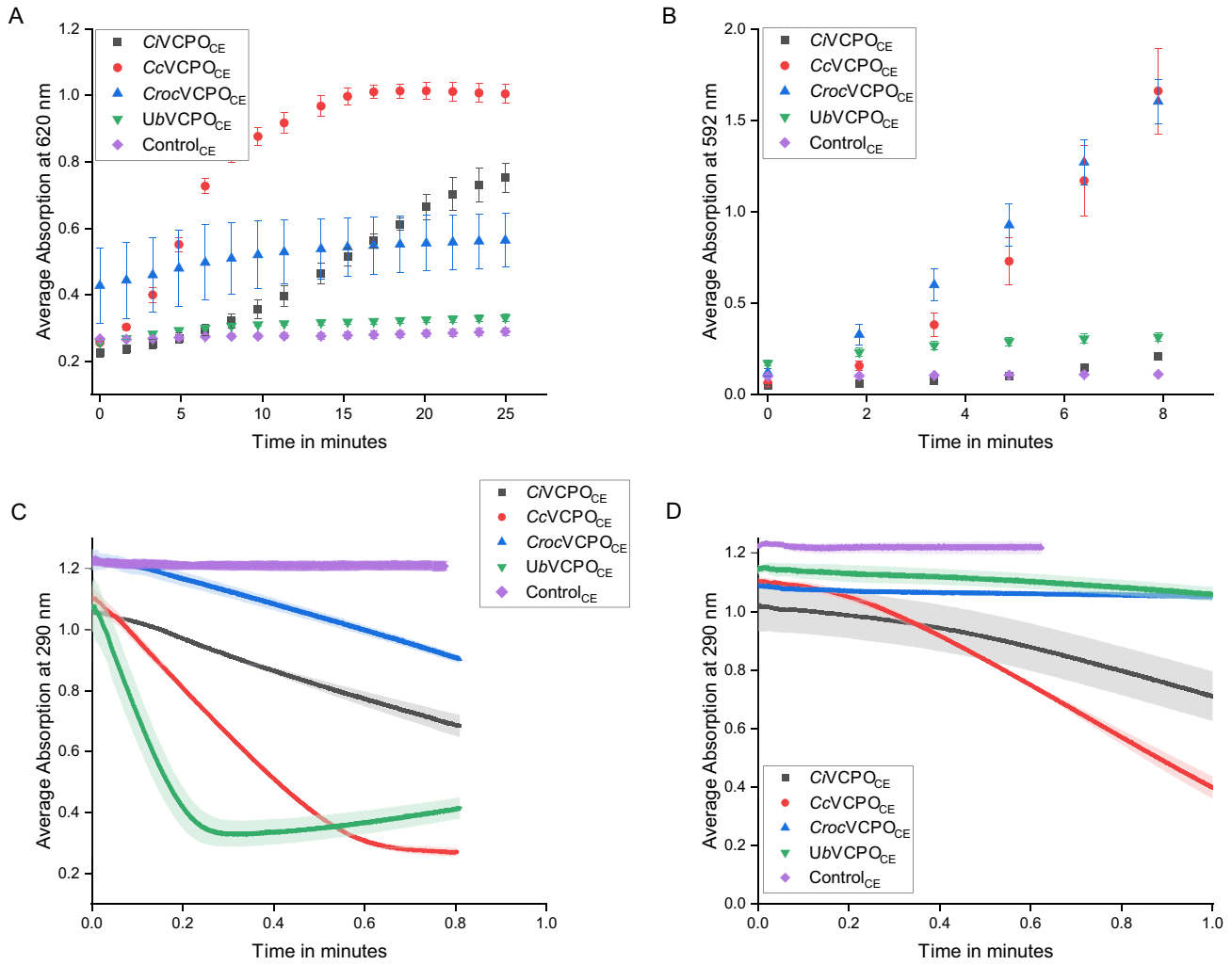

FIGURE 1 | Enzyme kinetic measurements using the crude extracts (CE) of the heterologous expressed enzymes *Ci*VCPO, *Cc*VCPO, *Croc*VCPO, U*b*VCPO, and the crude extract of a cultivation with the native *E. coli* BL21 (DE3) strain at room temperature ($n = 3$, technical replicates). (A) Thymol blue assay with potassium iodide (KI) as halide was performed in a 96-well plate with a total volume of 200 µL for 25 min, and the absorption was measured at 620 nm. (B) Phenol red assay with potassium bromide (KBr) as halide was performed in a 96-well plate with a total volume of 250 µL for 20 min and the absorption was measured at 592 nm. (C) MCD assay with KBr as halide performed with crude extracts in UV cuvettes with a total volume of 1 mL for 48 sec, and the absorption was measured at 290 nm. (D) MCD assay in UV cuvettes with potassium chloride (KCl) and the crude extracts, measured at 290 nm with a total volume of 1 mL for 1 min.

VCPOs can indeed be classified as chloroperoxidases. All variants and the reference enzyme were heterologous produced in the same *E. coli* strain BL21 (DE3). The native expression strain was used as negative control. All assays were carried out using crude extracts collected after cell lysis. The cultivations were conducted with the same cultivation conditions to allow direct comparison.

Thymol blue assay was conducted to confirm iodination activity (Figure 1A). Compared to the negative control, all putative VCPOs as well as the reference enzyme *Ci*VCPO showed higher product formation. In the initial phase, the fastest change in absorption was observed for catalysis by *Cc*VCPO which was exceeding that of the reference enzyme, whereas U*b*VCPO and *Croc*VCPO showed the lowest overall changes. The phenol red assay was conducted to check for bromination activity (Figure 1B). In this assay, the *Cc*VCPO again exhibits a very fast product formation in the initial phase compared to the reference enzyme. *Croc*VCPO exhibited a comparable slope. The *Ci*VCPO itself showed only a minor slope in contrast to the other enzymes. In both assays, U*b*VCPO starts at a higher absorption and reached saturation at an early time point. Both phenol red and thymol blue assays were only used for qualitative screenings because of halogenation at multiple carbon atom.

Quantitative bromination and chlorination activities were measured using monochlorodimedone (MCD) assay (Figure 1C,D). While the crude extract of the control showed no significant decrease in absorption for bromination reaction, all other tested crude extracts displayed substrate decrease over time. *Croc*VCPO and *Ci*VCPO exhibited nearly the same activity. The absorption for *Cc*VCPO and U*b*VCPO dropped much faster with U*b*VCPO being the most active one. The determination of chlorination activity showed a different pattern. *Cc*VCPO and *Ci*VCPO are the most active enzymes in this assay and U*b*VCPO and *Croc*VCPO only display a minor change in absorption. All three enzymes demonstrated halogenation activity with iodine, bromine, chlorine,

classifying them as chloroperoxidases. Interestingly, the data also indicate a distinct substrate preference, particularly in the bromination reactions. This could possibly be influenced by molecule size and substituent effects, which clearly distinguish the two substrates, MCD and phenol red, from each other.

2.3 | Enzyme Kinetic Parameters

To characterize kinetic parameters, the three VCPOs from a further expression run were additionally purified via their N-terminal his6x-tag using immobilized metal affinity chromatography (IMAC). The reference enzyme *Ci*VCPO was cultivated and purified identically. MCD assays were performed with varying concentrations of potassium bromide (KBr) or potassium chloride (KCl), respectively. Hydrogen peroxide was supplied in excess to secure pseudofirst-order reaction conditions with respect to the halide substrate. To calculate the kinetic parameters, substrate affinity constant (K_M), turnover number (k_{cat}), and the inhibitor affinity constant (K_I), a Michaelis–Menten equation with substrate inhibition was used and fitted by applying a nonlinear regression with the solver tool from Excel (Table 1). All three linearizations, Lineweaver–Burk, Eadie–Hofstee, and Hanes–Woolf, were applied and the mean value of these was taken as initial values for the nonlinear regression fitting.

The kinetic parameters for *Cc*VCPO and the reference enzyme *Ci*VCPO are similar to each other. This can be attributed to the close phylogenetic relation of the source organisms, resulting in high sequence and structural homology. An explanation for the slightly higher substrate affinity constants and consequently lower turnover numbers of *Cc*VCPO for both bromination and chlorination could be the substitution of Met_{216} in *Ci*VCPO to Lys_{216} in *Cc*VCPO. The amino acid is in both enzymes part of a loop region covering the binding pocket. The shift from the nonpolar methionine to a positively charged lysine may change the overall charge around the binding pocket as well as change the conformation and therefore the flexibility, resulting in a lower affinity of the enzyme to the substrate MCD.

The enzyme variant *Croc*VCPO displayed a low chlorination and bromination activity. Although its K_M values are comparable to the other tested enzymes. The turnover numbers are two orders of magnitude lower than the other enzyme variants with 1.77 and 0.21 s^{-1} for bromination and chlorination, respectively. Despite these modest kinetic parameters for the *Croc*VCPO variant, the phenol red assay with KBr clearly indicated that this variant exhibited high enzymatic activities for specific substrates.

The U*b*VCPO showed different kinetic behavior. While the phenol red and thymol blue assays suggested a modest iodination and bromination activity, in the MCD assays the U*b*VCPO variant exhibited bromination activity in the same range as *Ci*VCPO and *Cc*VCPO except for a lower substrate affinity constant of 0.009 mM. However, its chlorination activity reveals a high turnover number. To the authors knowledge, it is the highest turnover number measured for wild-type VCPO to date, although the K_M parameter is with 457.26 mM high compared to *Ci*VCPO with a K_M value of 1.91 mM.

2.4 | Biochemical Characterization

To further characterize the three VCPOs, all variants were tested with respect to temperature stability and solvent tolerance. To determine values for the characteristics, MCD assay with KBr as halide was used. Based on the previous results from the determination of the kinetic parameters, the concentration of KBr was switched from 500 μM to 100 μM which results in less substrate inhibition-influenced calculations.

Thermostability measurements after 1 h of incubation revealed that the fungal enzymes *Ci*VCPO and *Cc*VCPO retained a high catalytic activity up to 50°C. At 70°C, both enzymes experienced major activity loss of 36 % and 49 %, respectively. This characteristic behavior of *Ci*VCPOs is consistent with the findings of Van Schijndel et al. with the exception of an even higher thermostability of up to 80°C with an activity loss of 20 % [31].

TABLE 1 | Enzyme kinetic parameters obtained from MCD assay measurements with varying KBr and KCl concentrations, respectively. The enzymes were expressed, harvested, and purified via IMAC. The parameters were determined via nonlinear regression with substrate inhibited Michaelis–Menten equation. The assays for each KBr/KCl concentration were carried out in technical triplicates at room temperature. The k_{cat}/K_M values for *Ed*VCPO were calculated based on the K_M and k_{cat} values stated in the work of Tanaka et al. [21].

	K_M [mM]		k_{cat} [s^{-1}]		K_I [mM]		k_{cat}/K_M [$mM^{-1}\ s^{-1}$]	
Enzyme	**KBr**	**KCl**	**KBr**	**KCl**	**KBr**	**KCl**	**KBr**	**KCl**
*Ci*VCPO (this study)	$0.046^{-0.001}_{+0.001}$	$1.91^{-0.02}_{+0.02}$	$185.53^{-1.79}_{+2.01}$	$25.12^{-0.35}_{+0.35}$	$0.612^{+0.029}_{-0.029}$	$944.37^{-72.5}_{+78.5}$	$4.03*10^6$	$1.32*10^4$
*Cc*VCPO (this study)	$0.065^{+0.012}_{-0.009}$	$3.42^{-0.137}_{+0.141}$	$140.89^{-9.58}_{+7.07}$	$16.53^{-0.752}_{+0.743}$	$0.518^{-0.110}_{+0.135}$	$866.73^{-0.372}_{+1.616}$	$2.17*10^6$	$4.83*10^3$
*Croc*VCPO (this study)	$0.021^{-0.0006}_{+0.0007}$	$2.69^{-0.170}_{+0.217}$	$1.77^{-0.088}_{+0.091}$	$0.21^{-0.003}_{+0.004}$	$1.008^{-0.004}_{+0.004}$	$552.31^{-90.50}_{+101.88}$	$8.43*10^4$	$7.81*10^1$
U*b*VCPO (this study)	$0.009^{-0.001}_{+0.002}$	$457.26^{-92.1}_{+113.5}$	$179.86^{-2.42}_{+2.95}$	$511.07^{-131.31}_{+171.69}$	$0.876^{-0.548}_{+0.507}$	$25.48^{-5.25}_{+6.82}$	$2.00*10^7$	$1.12*10^3$
*Ci*VCPO [21, 29, 30]	0.009–0.015	$1.15*10^{-3}$–1.2	200–248	23	—	—	$1.3*10^7$–$2.8*10^7$	$2.0*10^4$
*Ed*VCPO [21]	0.005	1.2	60	2	—	—	$1.2*10^4$	$1.67*10^1$
*Hw*VCPO [17]	0.026	237	0.13	0.14	—	—	$4.94*10^3$	$5.91*10^{-1}$

This higher thermostability may be explained by the expression in the native organism with optimal expression conditions like proper folding by chaperons. In contrast, the bacterial VCPOs revealed a decreased thermostability compared to *Ci*VCPO and *Cc*VCPO. *Croc*VCPO exhibits a significant loss in activity already at 50°C. Particularly interesting is the behavior of U*b*VCPO at higher temperatures. This enzyme is heat activated at higher temperatures, e.g., 40°C of up to 181 % compared to its activity at room temperature. At higher temperatures then 40°C, the enzyme is completely deactivated with no measurable conversion at all. Such heat activation of a VCPO was likewise reported for *Ls*VHPO1 from the brown algae *Laminaria saccharina*. This enzyme exhibited a peak in iodination activity at 40 °C and a drastic loss in activity at higher temperatures [32].

The solvent tolerance assays show a similar behavior. The reference enzyme *Ci*VCPO proved a high tolerance toward an incubation in a 25 %(v/v) solvent concentration overnight (see Figure 2B). This characteristic property of the VCPO from *C. inaequalis* was already reported [7, 31]. Comparable to temperature stability results, the *Cc*VCPO showed a similar performance in bromination activity after incubation in different solvents. Dimethyl sulfoxide (DMSO) is the only solvent which significantly decreases the enzyme activity of all enzymes except for *Cc*VCPO. DMSO in higher concentration is known to destabilize the hydration shell of proteins. It destabilizes the tertiary and quaternary structure of proteins, and unfolds proteins [33, 34]. No residual activity was detected for *Croc*VCPO after incubation in DMSO. This may be explained by the hypothesis of a destabilization of a multimeric conformation of this enzyme variant. An indication for multimerization in *Croc*VCPO could be derived from the SDS gels (attached in the Supporting Information (SI)) presenting multiple bands in the gels. This particular pattern in the SDS gel was also observed for U*b*VCPO which unlike *Croc*VCPO still exhibits some activity after incubation in DMSO. Once again, the U*b*VCPO variant displays a particular behavior in solvent screening. Incubation in acetonitrile leads to a total loss in activity but in contrast to that the solvents ethanol and methanol activate the enzyme. The specific activities reached 127.5 % for incubation in ethanol and 158.8 % in methanol in relation to the catalysis with U*b*VCPO without incubation in an organic solvent. A similar behavior was detected for a laccase, DLac, from *Cerrena* sp. RSD1 after preincubation in solvents like acetone, methanol, ethanol, DMSO, and DMF, as well as for an elastase from *Pseudomonas aeruginosa* strain K and a protease from a halophilic *Bacillus* sp. EMB9 [35–37].

2.5 | Structural Analysis

To improve understanding of these new enzymes and explain their different characteristics, the predicted models of the enzyme monomers were generated from their native amino acid sequences by AlphaFold 3 and additionally superimposed onto the *Ci*VCPO crystal structure using ChimeraX 1.9 (Figure 3). Numerous studies showed the reliability of AlphaFold models for initial analysis and it was already used for studies on VHPOs [13, 17, 38–40]. However, it has to be stated that using AlphaFold 3 models only display preliminary insights into the structure of the presented enzymes. Experimental structure determination (e.g., crystallography) would provide a more accurate representation of the enzymes structure and enhance to allow for a comparison of higher quality. In general, the tertiary structure of VHPOs consisting of two four-helix bundles as well as the amino acids, which are directly involved in the reaction, is strongly conserved within this enzyme group. In contrast, the quaternary structures of VHPOs exhibit high diversity, varying from monomeric appearances, e.g., in case of VCPOs from *Curvularia*

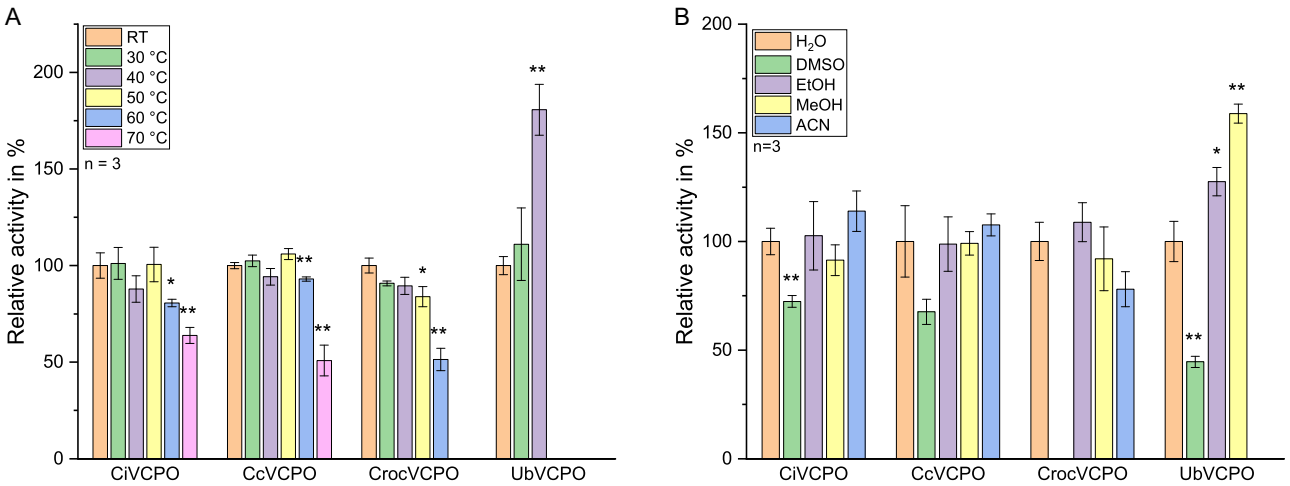

FIGURE 2 | Enzymatic activity of the purified *Cc*VCPO, *Croc*VCPO, and U*b*VCPO compared to *Ci*VCPO as reference in regard of thermostability and tolerance toward the solvents DMSO, ethanol, methanol, and acetonitrile determined by MCD assay with KBr as halide. (A) Thermostability was evaluated by the residually enzymatic activity in MCD assay after incubation for 1 h at varying temperatures from room temperature to 70°C. Experiments were conducted in technical triplicates. Resulting average activities are given in relation to the sample measured at room temperature. The *p*-value was calculated with a two-tailed, unpaired *t*-test. If the standard deviation showed a twofold difference between samples, the unequal *t*-test was performed (**p*-value ≤ 0.05; ***p*-value ≤ 0.01). (B) Tolerance toward solvents was evaluated by the residually enzymatic activity in MCD assay after incubation in 25 % solvent overnight. Experiments were conducted in technical triplicates. Resulting average activities are given in relation to the sample measured with water. The *p*-value was calculated with a two-tailed, unpaired *t*-test. If the standard deviation showed a twofold difference between samples, the unequal *t*-test was performed (**p*-value ≤ 0.05; ***p*-value ≤ 0.01).

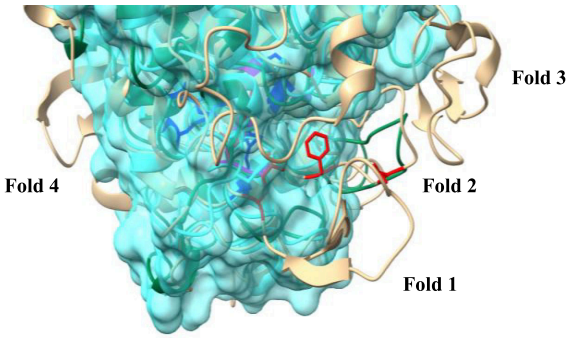

FIGURE 3 | Superimposition of modeled *Croc*VCPO (cyan blue) and U*b*VCPO (green) structures onto the *Ci*VCPO crystal structure (beige) with bound vanadate. The projected surface corresponds to *Croc*VCPO. Red amino acids indicate substrate-binding pocket residues in *Ci*VCPO not conserved across all characterized VCPOs. Magenta residues indicate conserved substrate-binding pocket residues, and dark blue residues indicate conserved active-site residues.

inaequalis to dimeric structures like the VBPO from *Ascophyllum nodosum* and dodecameric structures such as the VBPO from *Corallina pilulifera* [11].

All the predicted structures feature a conserved orientation and position of the conserved amino acids (Phe–Trp–Lys–Arg–His–Arg–Ser–His) in near proximity to the vanadate in the active site (results not shown). In addition, the enzymes show a conserved structure of the monomeric fold, although the sequence similarity is only 23 % for both bacterial VCPOs. The superimposition of the enzymes onto the structure of *Ci*VCPO revealed that some enzymes are lacking certain folds observed in the crystal structure of *Ci*VCPO. *Cc*VCPO displays all folds, but as already mentioned, has a crucial substituted amino acid in the fold covering the binding pocket. U*b*VCPO lacks the folds 1, 3, and 4, shown for *Ci*VCPO in Figure 3. It exhibits the fold 2 but only on secondary structure level. The amino acids themselves differ significantly, also with regard to important amino acids like Gln_{220}, His_{222}, and Asp_{390} that are relevant for substrate binding in *Ci*VCPO [10]. In U*b*VCPO, the positions of these three amino acids overlap with the amino acids Lys_{197}, Met_{199}, and Glu_{344}. In *Ci*VCPO, all these amino acids are polar. In comparison, the amino acid Met_{199} in U*b*VCPO deviates from this pattern. This amino acid has rather hydrophobic properties, which can lead to an altered substrate affinity of the enzyme. In addition, the amino acid Phe_{393} is completely missing in U*b*VCPO, which is also associated with substrate binding. *Croc*VCPO exhibits none of the four folds. The missing folds 1–3 covering the binding pocket, making the enzyme probably more prone to catalyze reactions with larger molecules such as thymol blue bearing three aromatic rings. The substrate itself may come in closer contact to the active site in this enzyme, enhancing the catalysis. Nevertheless, the MCD conversion is still very low, which contradicts this theory. A close look at the amino acids surrounding the active site reveals that the amino acids Gln_{220} and His_{222}, considered to be relevant for substrate binding, have been replaced by Phe_{187} and Leu_{211} in the enzyme variant *Croc*VCPO. A working hypothesis is that both hydrophobic residues, phenylalanine and leucine, may lead possibly to optimized hydrophobic conditions for an enhanced binding of hydrophobic substrates like thymol blue. Compared to thymol blue, which possess an estimated XlogP3 value of 6, MCD is significantly less hydrophobic with a XlogP3 value of 1.5 [41, 42]. The specific substrate affinity of the *Croc*VCPO variant aligns with the drastically reduced bromination and chlorination activity for this enzyme variant.

3 | Conclusion

In this study, three previously uncharacterized VCPOs were successfully expressed heterologous in *E. coli* and functionally validated. Two of the enzymes were described for the first time and one was only previously described regarding its bromination and sulfoxidation activity. The bacterial enzyme variant U*b*VCPO showed the highest reported chlorination turnover numbers for any wild-type VCPO described to date, combined with activation at 40°C and in the presence organic cosolvents such as ethanol and methanol. The structural analysis based on preliminary enzyme modeling generated with AlphaFold 3 revealed a conserved active-site architecture. The amino acids surrounding the active site, however, differ greatly in some instances, particularly for the bacterial variants *Croc*VCPO and U*b*VCPO. These findings broaden the toolbox of sustainable biocatalysts for versatile halogenation reactions with distinct, industrially relevant properties.

4 | Experimental Section

4.1 | Strain Construction

The DNA sequences of the enzymes were codon optimized for expression in *E. coli* BL21 (DE3) and synthesized by Twist Bioscience (South San Francisco, USA) and provided in pET blank (Amp) plasmids. Via Gibson assembly using Q5 high fidelity master mix (M0492L, New England BioLabs Inc.) and 2X NEBuilder HiFi DNA Assembly Master Mix (E2621L, New England BioLabs Inc.), a gIII-signal peptide (codon optimized for *E. coli*) from the filamentous phage fd gene III and a his6x-tag sequence was cloned in frame upstream of the gene of interest.

4.2 | Heterologous Protein Expression

100 mL precultures in LB medium containing 100 µg/mL ampicillin were inoculated and incubated over night at 37°C and 180 rpm. For the main culture, 200 mL TB medium containing 100 µg/mL ampicillin was inoculated with the preculture to an optical density of 0.04 and incubated at 37 °C and 180 rpm. After growth to an optical density of 0.4–0.8, the protein expression was induced by adding 50 µM IPTG and 2 % (v/v) ethanol. The cultures were incubated for another 24 h at a reduced temperature of 25°C and 180 rpm. The harvest was performed by centrifugation of the cultures at 4528 xg, 4°C for 30 min. The supernatant was discarded, and the pellet was stored at −20 °C.

4.3 | Cell Disruption and Enzyme Recovery

The pellets were resuspended each in 15 mL of 50 mM Tris/H_2SO_4 pH 8.1 buffer. One spatula tip of lysozyme (62971-10G-F, Sigma-Aldrich Co.), DNaseI (10104159001, Roche Diagnostics

GmbH), 1 tablet of protease inhibitor cocktail (04693159001, Roche Diagnostics GmbH), and one spatula tip of $MgSO_4 \cdot 7\,H_2O$ were added and the solution was incubated by gently rotating for 30 min at 4°C. The cells were subsequently sonicated three times for 5 min with 20 s intervals and an amplitude of 80%. The lysate was centrifuged at 4528 xg, 4°C for 30 min. The supernatant was transferred into Amicon Ultra-15 centrifugal filter devices with a cutoff at 30 kDa (UFC903008, Merck KGaA). The retentate of the concentration step was then washed in the same filter system with 9 mL 50 mM Tris/H_2SO_4 pH 8.1 buffer containing 1 mM Na_3VO_4. The enzymes were stored at 4°C for short-term storage and at −20°C with 20 %(v/v) glycerol for long-term storage.

4.4 | Enzyme Purification

The his6x-tagged enzymes were purified by using His-trap chromatography. The cells were lysed as described above for enzyme concentration. The buffer used for cell lysis was supplemented with 1 mM Na_3VO_4 and 30 mM Imidazole. The lysates were centrifuged at 33 152 xg, 4°C for 1 h. IMAC for protein purification was performed using an ÄKTA start (Cytiva Life Sciences, USA) with protein detection at 280 nm with an HisTrap High Performance 1 mL column (GE29-0510−21, Cytiva Life Sciences, USA). The lysate buffer with 30 mM imidazole was also used for column loading of the sample. As elution buffer, 50 mM Tris/H_2SO_4 pH 8.1 buffer containing 1 mM Na_3VO_4 and 500 mM imidazole was used. The pooled enzyme fractions were washed using the Amicon Ultra-15 centrifugal filter devices with a cut-off at 30 kDa (UFC903008, Merck KGaA) with 9 mL 50 mM Tris/H_2SO_4 pH 8.1 buffer containing 1 mM Na_3VO_4.

4.5 | Enzyme Assays

Protein concentrations were determined via Bradford assay using bovine serum albumin (BSA) as a protein standard. To check for the enzymes in the sample, SDS-page was performed to examine for proteins of the expected size on Mini PROTEAN TGX gels (Bio-Rad Laboratories Inc.). The protein samples were loaded with 1X Laemmli sample buffer (1610747, Bio-Rad Laboratories Inc.). A preliminary step of heating at 95°C for 5 min was done before electrophoresis. The proteins were visualized by staining the gel with 0.2 % Coomassie blue solution for 30 min and subsequent destaining in Millipore water overnight. The following description for the assays for the determination of enzyme activity is giving a short overview. Detailed information concerning stock and final concentrations of the used components are listed in the SI.

The bromination of phenol red to bromophenol blue was used to screen for bromination activity of the enzymes. The assay consisted of 80 µL 0.5 mM phenol red, 20 µL 50 mM KBr, 50 µL 20 mM H_2O_2, 1 µL of enzyme concentrate or 10 µL enzyme crude extract, and 1 M citrate buffer pH 5.0 with 1 mM Na_3VO_4 to a total volume of 250 µL. The reaction was started by adding H_2O_2. The absorbance was measured with an Infinite M200 pro reader (Tecan Trading AG, Switzerland) at 592 nm for 20 min. The reactions were performed at room temperature in triplicates.

The iodination activity of the enzymes was determined qualitatively by monitoring the reaction of thymol blue to diiodothymolsulfophtalein. The resulting product was measured with an Infinite M200 pro reader (Tecan Trading AG, Switzerland) at an absorption of 620 nm for 25 min. The assay consisted of 20 µL 1 mM Thymol blue resolved in ethanol and denatured with methylethylketone, 4 µL 200 mM KI, 20 µL 1 mM H_2O_2, 1 µL of enzyme concentrate or 10 µL enzyme crude extract, and 100 mM phosphate buffer pH 8.0 with 1 mM Na_3VO_4 to a total volume of 200 µL. The reaction was started by adding H_2O_2. The reactions were performed at room temperature in triplicates.

Quantitative determination of bromination and chlorination activity was conducted via the monochlorodimedone (MCD) assay. The assay comprised 100 µL of 0.5 mM MCD, 5 µL of 1 mM KBr or KCl, 100 µL of 50 mM H_2O_2, 10 µL of the sample, including enzymes, 100 µL of 1 M citrate buffer pH 5.0 containing 1 mM Na_3VO_4, and water to make up a total volume of 1 mL. The reaction was initiated by adding the H_2O_2. Absorbance was measured in UV cuvettes at 290 nm by a Cary 60 UV/Vis spectrophotometer (Agilent Technologies, United States) at room temperature and executed in triplicates for 2 min. The resulting activity was calculated using the MCD extinction coefficient $\varepsilon_{290\ nm} = 0.0199\,M^{-1}\,cm^{-1}$ [43].

To obtain kinetic parameters for bromination and chlorination activity of the VCPOs, the MCD assay was carried out with varying KBr (0 µM to 1 mM KBr) and KCl (0 mM to 500 mM KCl) concentrations. All measurements were performed as triplicates. As substrate inhibition was observed, the data were fitted in a nonlinear regression for the Michaelis–Menten equation considering substrate inhibition using the solver tool from Excel (Microsoft Corporation) to reliably estimate K_M and k_{cat}. The solver was used to minimize the estimate of goodness calculated for the estimated values compared to the measured values. The calculated values of the fitted data compared to the measured values are shown in the SI.

4.6 | Enzyme Structure Analysis

Structures of the native amino acid sequence from the putative VCPOs were predicted with the AlphaFold 3 Server Beta. For visualization, the predicted model from AlphaFold was inserted into ChimeraX 1.9 and was used to visualize enzymes. Relevant amino acid residues, potential binding pockets, or substrate tunnels were visualized using coloring and depiction tools. To investigate and compare the reactive sites of the putative VCPOs, ChimeraX was used to superimpose the enzymes for better comparison of predicted positioning of relevant amino acids in the binding pockets or reactive sites using the matchmaker tool.

Acknowledgments

The authors acknowledge the support by Proteineer GmbH. We also thank Prof. Johannes Kabisch and Aron Eiermann for helping with the sequence-based research.

Open Access funding enabled and organized by Projekt DEAL.

Conflicts of Interest

The authors declare no conflicts of interest.

Data Availability Statement

The data that support the findings of this study are available from the corresponding author upon reasonable request.

References

1. R. Lin, A. P. Amrute, and J. Pérez-Ramírez, "Halogen-Mediated Conversion of Hydrocarbons to Commodities," *Chemical Reviews* 117, no. 5 (2017): 4182–4247, https://doi.org/10.1021/acs.chemrev.6b00551.

2. P. Jeschke, "Recent Developments in Fluorine-Containing Pesticides," *Pest Management Science* 80, no. 7 (2024): 3065–3087, https://doi.org/10.1002/ps.7921.

3. D. Benedetto Tiz, M. D'Alì, N. Iraci, C. Santi, and L. Sancineto, "Halogen-Containing Drugs in 2025: A Record Year for the Therapeutic Use and Synthesis of FDA-Approved Small Molecules," *Biomolecules* 16, no. 3 (2026): 381, https://doi.org/10.3390/biom16030381.

4. Y. Fu, H. Li, C. Xu, et al., "Selective Chemoenzymatic Synthesis of Diverse Halo-Compounds by Vanadium-Dependent Haloperoxidase," *ChemCatChem* 17, no. 12 (2025): e202500584, https://doi.org/10.1002/cctc.202500584.

5. A. Butler and M. Sandy, "Mechanistic Considerations of Halogenating Enzymes," *Nature* 460, no. 7257 (2009): 848–854, https://doi.org/10.1038/nature08303.

6. G. T. Höfler, A. But, and F. Hollmann, "Haloperoxidases as Catalysts in Organic Synthesis," *Organic & Biomolecular Chemistry* 17, no. 42 (2019): 9267–9274, https://doi.org/10.1039/C9OB01884K.

7. E. Fernández-Fueyo, M. van Wingerden, R. Renirie, et al., "Chemoenzymatic Halogenation of Phenols by Using the Haloperoxidase from *Curvularia Inaequalis*," *ChemCatChem* 7 (2015): 4035–4038, https://doi.org/10.1002/cctc.201500862.

8. F. H. Vaillancourt, E. Yeh, D. A. Vosburg, S. Garneau-Tsodikova, and C. T. Walsh, "Nature's Inventory of Halogenation Catalysts: Oxidative Strategies Predominate," *Chemical Reviews* 106, no. 8 (2006): 3364–3378, https://doi.org/10.1021/cr050313i.

9. R. Wever, B. Krenn, and R. Renirie, "Marine Vanadium-Dependent Haloperoxidases, Their Isolation, Characterization, and Application." *Methods in Enzymology* 605 (2018): 141–201, https://doi.org/10.1016/bs.mie.2018.02.026.

10. E. F. Gérard, T. Mokkawes, L. O. Johannissen, et al., "How Is Substrate Halogenation Triggered by the Vanadium Haloperoxidase from *Curvularia Inaequalis*?," *ACS Catalysis* 13, no. 12 (2023): 8247–8261, https://doi.org/10.1021/acscatal.3c00761.

11. J. Latham, E. Brandenburger, S. A. Shepherd, B. R. K. Menon, and J. Micklefield, "Development of Halogenase Enzymes for Use in Synthesis," *Chemical Reviews* 118, no. 1 (2018): 232–269, https://doi.org/10.1021/acs.chemrev.7b00032.

12. P. Y.-T. Chen, S. Adak, J. R. Chekan, et al., "Structural Basis of Stereospecific Vanadium-Dependent Haloperoxidase Family Enzymes in Napyradiomycin Biosynthesis." *Biochemistry* 61 (2022): 1844–1852, https://doi.org/10.1021/acs.biochem.2c00338.

13. P. Zeides, K. Bellmann-Sickert, R. Zhang, et al., "Unraveling the Molecular Basis of Substrate Specificity and Halogen Activation in Vanadium-Dependent Haloperoxidases," *Nature Communications* 16, no. 1 (2025): 2083, https://doi.org/10.1038/s41467-025-57023-1.

14. Z. Chen, "Recent Development of Biomimetic Halogenation Inspired by Vanadium Dependent Haloperoxidase," *Coordination Chemistry Reviews* 457 (2022): 214404, https://doi.org/10.1016/j.ccr.2021.214404.

15. B. Chen, Y. Zeng, J. Sha, et al., "Vanadium-Dependent Haloperoxidases: Recent Advances and Perspectives," *Biotechnology Advances* 87 (2026): 108797, https://doi.org/10.1016/j.biotechadv.2026.108797.

16. H. Vilter, "Peroxidases from Phaeophyceae: A Vanadium(V)-Dependent Peroxidase from *Ascophyllum Nodosum*," *Phytochemistry* 23, no. 7 (1984): 1387–1390, https://doi.org/10.1016/S0031-9422(00)80471-9.

17. B. Cochereau, Y. Le Strat, Q. Ji, et al., "Heterologous Expression and Biochemical Characterization of a New Chloroperoxidase Isolated from the Deep-Sea Hydrothermal Vent Black Yeast, *Hortaea Werneckii*, UBOCC-A-208029," *Marine Biotechnology* 25 (2023): 519–536, https://doi.org/10.1007/s10126-023-10222-7.

18. S. M. K. McKinnie, Z. Miles, and B. Moore, "Characterization and Biochemical Assays of, *Streptomyces*, Vanadium-Dependent Chloroperoxidases." *Methods in Enzymology* 604 (2018): 405–424, https://doi.org/10.1016/bs.mie.2018.02.016.

19. J.-B. Fournier, E. Rebuffet, L. Delage, et al., "The Vanadium Iodoperoxidase from the Marine, *Flavobacteriaceae*, Species, *Zobellia Galactanivorans*, Reveals Novel Molecular and Evolutionary Features of Halide Specificity in the Vanadium Haloperoxidase Enzyme Family," *Applied and Environmental Microbiology* 80 (2014): 7561–7573, https://doi.org/10.1128/aem.02430-14.

20. A. Messerschmidt and R. Wever, "X-Ray Structure of a Vanadium-Containing Enzyme: Chloroperoxidase from the Fungus *Curvularia Inaequalis*." *Proceedings of the National Academy of Sciences* 93, no. 1 (1996): 392–396, https://doi.org/10.1073/pnas.93.1.392.

21. P. Barnett, W. Hemrika, H. L. Dekker, A. O. Muijsers, R. Renirie, and R. Wever, "Isolation, Characterization, and Primary Structure of the Vanadium Chloroperoxidase from the Fungus *Embellisia Didymospora*," *Journal of Biological Chemistry* 273, no. 36 (1998): 23381–23387, https://doi.org/10.1074/jbc.273.36.23381.

22. H. Li, P. Duan, Y. Huang, et al., "Vanadium-Containing Chloroperoxidase-Catalyzed Versatile Valorization of Phenols and Phenolic Acids," *ACS Catalysis* 14, no. 3 (2024): 1733–1740, https://doi.org/10.1021/acscatal.3c05333.

23. J. J. Dong, E. Fernández-Fueyo, J. Li, et al., "Halofunctionalization of Alkenes by Vanadium Chloroperoxidase from *Curvularia Inaequalis*," *Chemical Communications* 53, no. 46 (2017): 6207–6210, https://doi.org/10.1039/C7CC03368K.

24. S. Bormann, M. M. C. H. van Schie, T. P. De Almeida, et al., "H_2O_2 Production at Low Overpotentials for Electroenzymatic Halogenation Reactions," *ChemSusChem* 12, no. 21 (2019): 4759–4763, https://doi.org/10.1002/cssc.201902326.

25. H. J. Lee, C. U. Brzezinski, S. A. Solis, et al., "Oxidative Rearrangement of Indoles Enabled by Promiscuous Cryptic Halogenation with Vanadium-Dependent Haloperoxidases," *ACS Catalysis* 16, no. 3 (2026): 2606–2614, https://doi.org/10.1021/acscatal.5c07839.

26. E. J. Gross, S. G. Barthel, C. U. Brzezinski, L. Z. Hessefort, J. Bacsa, and K. F. Biegasiewicz, "Chlorination of Amines by a Vanadium-Dependent Chloroperoxidase," *ACS Catalysis* 16 (2026): 6241-6246, https://doi.org/10.1021/acscatal.6c00816.

27. Y.-H. Zhang, Y.-T. Zou, Y.-Y. Zeng, L. Liu, and B.-S. Chen, "Enantioselectivity in Vanadium-Dependent Haloperoxidases of Different Marine Sources for Sulfide Oxidation to Sulfoxides," *Marine Drugs* 22, no. 9 (2024): 419, https://doi.org/10.3390/md22090419.

28. T. Loan, A. Karpe, S. Babaei, et al., "Biosynthesis of Bromoform by *Curvularia Fungi* Provides a Natural Pathway to Mitigate Enteric Methane Emissions from Ruminants," *Biotechnology Reports* 45 (2025): e00876, https://doi.org/10.1016/j.btre.2025.e00876.

29. W. Hemrika, R. Renirie, S. Macedo-Ribeiro, A. Messerschmidt, and R. Wever, "Heterologous Expression of the Vanadium-Containing Chloroperoxidase from *Curvularia Inaequalis* in *Saccharomyces Cerevisiae* and Site-Directed Mutagenesis of the Active Site Residues His496, Lys353, Arg360, and Arg490," *Journal of Biological Chemistry* 274, no. 34 (1999): 23820–23827, https://doi.org/10.1074/jbc.274.34.23820.

30. N. Tanaka, Z. Hasan, and R. Wever, "Kinetic Characterization of Active Site Mutants Ser402Ala and Phe397His of Vanadium Chloroperoxidase

from the Fungus *Curvularia Inaequalis*," *Inorganica Chimica Acta* 356 (2003): 288–296, https://doi.org/10.1016/S0020-1693(03)00476-6.

31. J. W. P. M. Van Schijndel, P. Barnett, J. Roelse, E. G. M. Vollenbroek, and R. Wever, "The Stability and Steady-State Kinetics of Vanadium Chloroperoxidase from the Fungus *Curvularia Inaequalis*," *European Journal of Biochemistry* 225, no. 1 (1994): 151–157, https://doi.org/10.1111/j.1432-1033.1994.00151.x.

32. M. Almeida, S. Filipe, M. Humanes, et al., "Vanadium Haloperoxidases from Brown Algae of the *Laminariaceae* Family," *Phytochemistry* 57, no. 5 (2001): 633–642, https://doi.org/10.1016/S0031-9422(01)00094-2.

33. T. Arakawa, Y. Kita, and S. N. Timasheff, "Protein Precipitation and Denaturation by Dimethyl Sulfoxide," *Biophysical Chemistry* 131, no. 1–3 (2007): 62–70, https://doi.org/10.1016/j.bpc.2007.09.004.

34. A. Czajlik, Á. Batta, K. Kerner, et al., "DMSO-Induced Unfolding of the Antifungal Disulfide Protein PAF and Its Inactive Variant: A Combined NMR and DSC Study," *International Journal of Molecular Sciences* 24, no. 2 (2023): 1208, https://doi.org/10.3390/ijms24021208.

35. M.-H. Wu, M.-C. Lin, C.-C. Lee, S.-M. Yu, A. H.-J. Wang, and T.-H. D. Ho, "Enhancement of Laccase Activity by Pre-Incubation with Organic Solvents," *Scientific Reports* 9, no. 1 (2019): 9754, https://doi.org/10.1038/s41598-019-45118-x.

36. R. Sinha and S. K. Khare, "Effect of Organic Solvents on the Structure and Activity of Moderately Halophilic, Bacillus sp. EMB9 Protease," *Extremophiles : Life Under Extreme Conditions* 18, no. 6 (2014): 1057–1066, https://doi.org/10.1007/s00792-014-0683-4.

37. R. N. Z. R. Abd. Rahman, A. B. Salleh, M. Basri, and C. F. Wong, "Role of α-Helical Structure in Organic Solvent-Activated Homodimer of Elastase Strain K," *International Journal of Molecular Sciences* 12, no. 9 (2011): 5797–5814, https://doi.org/10.3390/ijms12095797.

38. T. C. Terwilliger, D. Liebschner, T. I. Croll, et al., "AlphaFold Predictions Are Valuable Hypotheses and Accelerate but Do Not Replace Experimental Structure Determination," *Nature Methods* 21, no. 1 (2024): 110–116, https://doi.org/10.1038/s41592-023-02087-4.

39. S. K. Mahtha, S. Venkadesan, and D. Mohanty, "Comparative Evaluation of the Prediction Accuracy of AlphaFold and ESMFold for Monomeric and Dimeric Proteins," *NAR Genomics and Bioinformatics* 8, no. 1 (2026): lqag002, https://doi.org/10.1093/nargab/lqag002.

40. J. T. Baumgartner, C. S. McCaughey, H. S. Fleming, A. R. Lentz, L. M. Sanchez, and S. M. K. McKinnie, "Vanadium-Dependent Haloperoxidases from Diverse Microbes Halogenate Exogenous Alkyl Quinolone Quorum Sensing Signals," *Biochemistry* (2024), https://doi.org/10.1101/2024.07.31.606109.

41. Bethesda (MD): National Library of Medicine (US), National Center for Biotechnology Information, "*PubChem Compound Summary for CID. 65565, Thymol Blue', PubChem*," Accessed Dec 2025.https://pubchem.ncbi.nlm.nih.gov/compound/Thymol-Blue.

42. Bethesda (MD): National Library of Medicine (US), National Center for Biotechnology Information, "*PubChem Compound Summary for CID. 122278, Chlorodimedone, PubChem*," Accessed Dec 2025. https://pubchem.ncbi.nlm.nih.gov/compound/Chlorodimedone,

43. R. R. Everett, H. S. Soedjak, and A. Butler, "Mechanism of Dioxygen Formation Catalyzed by Vanadium Bromoperoxidase. Steady State Kinetic Analysis and Comparison to the Mechanism of Bromination." *Journal of Biological Chemistry* 265, no. 26 (1990): 15671–15679, https://doi.org/10.1016/S0021-9258(18)55451-X.

44. National Library of Medicine - Naltional Center for Biotechnology Information, Accessed Jan 2026.https://www.ncbi.nlm.nih.gov/nuccore/.

45. UniProt, Accessed Jan 2026. https://www.uniprot.org/align/clustalo-R20260103-151013-0313-90697957-p1m/overview.

46. J. W. P. M. Van Schijndel, E. G. M. Vollenbroek, and R. Wever, "The Chloroperoxidase from the Fungus *Curvularia Inaequalis*; a Novel Vanadium Enzyme," *Biochimica et Biophysica Acta (BBA) - Protein Structure and Molecular Enzymology* 1161, no. 2-3 (1993): 249–256, https://doi.org/10.1016/0167-4838(93)90221-C.

Supporting Information

Additional supporting information can be found online in the Supporting Information section.